

Conclusion: A novel time-division cell multiplexer that can generate time-multiplexed ultrafast optical cells with minimal hardware was presented. In the fundamental experiment, generation of a 40 Gbit/s optical cell was demonstrated. With its ultrafast performance and minimal hardware, this cell multiplexer will play an important role in the future photonic ATM cell switch.

Acknowledgment: The authors wish to thank Dr. K. Yuki-matsu and Mr. S. Kikuchi for their encouragement and discussions.

M. TSUKADA
Y. SHIMAZU

7th September 1990

NTT Communication Switching Laboratories
9-11 Midori-cho 3-chome
Musashino-shi Tokyo 180 Japan

References

- 1 KUROYANAGI, S., SHIMO, T., and MURAKAMI, K.: 'Photonic ATM switching network'. Int. Topical Meeting Photonic Switching, 1990, 14B-2, pp. 223-225
- 2 SHIMAZU, Y., TSUKADA, M., and KIKUCHI, S.: 'Ultrafast photonic packet switch with optical output buffer'. Int. Topical Meeting Photonic Switching, 1990, 14B-1, pp. 220-222
- 3 TAKADA, A., SUGIE, T., and SARUWATARI, M.: 'High-speed picosecond optical pulse compression from gain-switched 1.3 μ m distributed feedback laser diode (DFB-LD) through highly dispersive single-mode fiber'. *J. Lightwave Technol.*, 1987, LT-5, pp. 1525-1533
- 4 TERUI, H., KOMINATO, T., and KOBAYASHI, M.: 'Lossless 1 \times 4 laser diode optical gate switch'. CLEO, 1990, CTUF4
- 5 NAGARAJAN, R., KAMIYA, Y., KASUKAWA, A., and OKAMOTO, H.: 'Observation of ultrashort (<4 ps) gain-switched optical pulses from long-wavelength multiple quantum well lasers'. *Appl. Phys. Lett.*, 1989, 55, pp. 1273-1275

APPLICATION OF THE FD-TD METHOD TO THE ANALYSIS OF H-PLANE WAVEGUIDE DISCONTINUITIES

Indexing terms: Waveguides, Electromagnetic waves

A direct finite-difference time-domain (FD-TD) method is applied to the analysis of waveguide discontinuities. Both the validity and efficiency of the method are demonstrated in the case of an H-plane right-angle corner bend with and without dielectric loading. Comparisons of the present results with those obtained using the spectral-domain methods are made and they are shown to be in good agreement.

Introduction: Maxwell's time-dependent differential equations can be represented by a set of difference equations that can be solved numerically using a digital computer. This procedure is referred to as the finite-difference time-domain (FD-TD) method. This approach for solving electromagnetic problems is straightforward and can be easily adapted to complex geometries. It has been applied to problems of scattering,¹ microstrip components,² antenna radiation, etc. There has been no application of the method to waveguide discontinuities analysis. This is because of the complexity of the dispersion relation and the fact that the waveguide has a high Q factor. The FD-TD method is used to analyse the waveguide discontinuities. The main issues are presented in the following:

Excitation choice: The excitation that will be used on the excitation plane consists of a monochromatic dominant TE₁₀ mode wave of unit amplitude

$$E_z = \sin(2\pi f t) \sin\left(\frac{\pi y}{W}\right) \quad (1)$$

Here f is the source frequency which is chosen to lie in the

working band of the dominant mode and W is the width of the waveguide port.

Boundary truncation: Boundary truncation must be used to carry out numerical simulation of the out-going waves at the end plane and the source plane. If the separation between the end plane and the discontinuity is one waveguide wavelength, λ_g , only the dominant mode appears near the boundary. In this case the wave will approach the end wall at normal incidence with the dominant mode phase velocity, v_p . This means that the tangential fields on the outer boundary will obey the one-dimensional wave equation along the direction normal to the mesh wall, which can be written as

$$\left(\frac{\partial}{\partial x} - \frac{1}{v_p} \frac{\partial}{\partial t}\right) E_{tan} = 0 \quad (2)$$

This equation is easily discretised using only field components on and just inside the mesh wall, yielding the difference equation

$$E_M^n = E_{M-1}^{n-1} + \frac{v_p \Delta t - \Delta x}{v_p \Delta t + \Delta x} (E_M^{n-1} - E_{M-1}^n) \quad (3)$$

where E_M represents the tangential electric field components on the boundary and E_{M-1} represents the tangential electric field components a distance of one node inside the boundary.

For the source plane, the boundary treatment is different from that of the end plane because, besides an out-going wave being reflected from the discontinuity, there is a source incident wave. We treat this boundary using the following procedure: (1) the total field everywhere except on the source plane is computed, (2) the scattered field on one node inside the source plane is derived by subtracting the known incident field from the computed total field, (3) the absorbing boundary condition eqn. 3 is applied to the scattered field on the outer boundary, and (4) the total field on the source plane is computed by summing the known incident field and the scattered field which was obtained in the third step.

Field component calculation and frequency parameter extraction: Yee's FD-TD method³ was employed to solve Maxwell's equations. Starting with the excitation eqn. 1 and assuming that the initial field is zero, the fields within the computation domain can be evaluated. After the fields on the reference planes reach the steady-state, their amplitudes and phase are determined directly from the time-domain waveforms. Once the total field distribution across the reference plane is obtained, the dominant mode component can be calculated using the orthogonal property of the waveguide mode.

Numerical result: Using the above method, analysis was carried out on a right-angle waveguide corner configured with and without dielectric loading. In Fig. 1, the starts are the

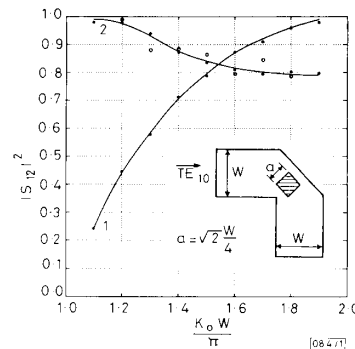


Fig. 1 Power transmission coefficient of right angle corner bend

- 1 without dielectric loading
- 2 with dielectric loading $\epsilon_r = 2.1$

FD-TD results. The results are in good agreement with that obtained by the spectral-domain methods, shown by the solid line¹ and the solid line², and experiment data,¹ presented by the circular dots.

Fig. 2 shows the electric field time response on a reference plane. From this Figure, we see that it takes a long time for the fields in the waveguide to become steady. This is because of the high Q property of the waveguide.

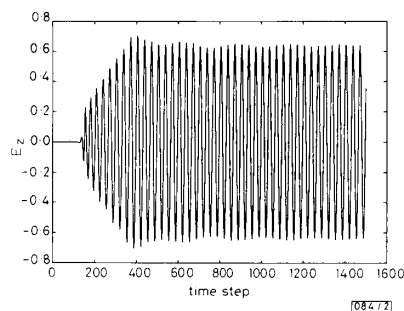


Fig. 2 Time waveform of E_z

Conclusion: The H-plane waveguide discontinuities have been analysed using the FD-TD method. The results are in good agreement with those from the spectral-domain analysis methods^{1,2} and the experimental data.¹

In our calculation, we choose a monochromatic wave as the excitation. This method requires an individual FD-TD run for every frequency of interest. An alternative approach is to implement FD-TD using a non-monochromatic wave excitation and take the Fourier transform of the time-domain waveforms to obtain the frequency response in a broad band from a single FD-TD run. These two methods have different advantages. The results obtained with the second excitation will be published in a separate paper.

Z.-Q. BI
K.-L. WU
J. LITVA

31st August 1990

Communications Research Laboratory
McMaster University
Ontario, Canada, L8S 4K1

References

1. WU, K. L., DELISLE, G. Y., FANG, D. G., and LECOUR, M.: 'Waveguide discontinuity analysis with a coupled finite-boundary element method', *IEEE Trans.*, 1989, **MTT-37**, pp. 993-998
2. KOSHIBA, M., SATO, M., and SUZUKI, M.: 'Application of finite-element method to H-plane waveguide discontinuities', *Electron. Lett.*, 1982, **18**, pp. 364-365
3. TAFLOVE, A., and UMASHANKAR, K. R.: 'Review of FD-TD numerical modeling of electromagnetic wave scattering and radar cross section', *Proc. IEEE*, 1989, **77**, pp. 682-699
4. ZHANG, X., and MEL, K. K.: 'Time-domain finite difference approach to the calculation of the frequency-dependent characteristics of microstrip discontinuities', *IEEE Trans.*, 1988, **MTT-36**, pp. 1775-1787
5. YEE, K. S.: 'Numerical solution of initial boundary value problems involving Maxwell's equations in isotropic media', *IEEE Trans.*, 1966, **AP-14**, pp. 302-307

CARRIER LIFETIME INCREASE IN SILICON BY GETTERING WITH A MeV-IMPLANTED CARBON-RICH LAYER

Indexing terms: Carrier lifetime, Silicon

The gettering efficiency of silicon implanted with carbon ions in the energy range 0.33-10 MeV was tested by carrier lifetime measurements. After an intentional contamination of the sample back side with gold as a lifetime killer, we found values for the generation lifetime of the minority carriers on the front side higher by 1-2 orders of magnitude as compared with unimplanted silicon.

Introduction: The use of ion implantation to modify the dopant distribution in single crystalline silicon and other semiconductors is widely accepted in semiconductor technology. The implantation of nondopant elements has also been paid much attention. The formation of silicon-on-insulator structures by ion beam synthesis and the introduction of damaged regions to perform gettering are examples of this type.¹⁻³

Beyond high dose implantation and the use of nondopant elements, much effort has been devoted to the use of high implantation energies above 200 keV up to several MeV to produce materials with better and/or new properties. An interesting new technique to produce a region in a silicon wafer being able to getter metallic impurities very near to the active device region was proposed by Wong *et al.*⁴ High energy implantation of oxygen or carbon with an energy of up to 4 MeV and a dose in the range of 10^{16} cm^{-2} was used to create a buried damaged region with a remarkable gettering efficiency of the additionally introduced gold. Wong *et al.*, called this process 'proximity gettering'. Up to now, this effect was only proved by means of measuring the atomic profile by secondary ion mass spectroscopy (SIMS).

We present a test of the gettering efficiency by measurement of the carrier lifetime. Carbon implantation was used to

produce damage region because this type of MeV-implantation was found to be more effective in gettering than oxygen.*

Experimental: Silicon wafers ($\langle 100 \rangle$, n -type, 3-5 $\Omega \text{ cm}$, 2") manufactured from a Czochralski-grown crystal were annealed at 1100°C for 4 h in dry nitrogen to create a surface region of 4 μm denuded in oxygen. A silicon dioxide layer was grown at 1000°C in dry oxygen to a thickness of 100 nm. After thinning the oxide on the lapped backside of the sample to a thickness of 30 nm by chemical etching, gold was implanted into the backside with an energy of 330 keV and a dose of 10^{12} cm^{-2} . In this manner gold was used as a lifetime killer to illustrate the gettering effect of the carbon implanted layer.

Carbon was then implanted at energies of 0.33, 2.4 and 10 MeV and a dose of 10^{16} cm^{-2} at room temperature. The implantation at 0.33 MeV was performed by a conventional implanter. For the implantation at the higher energies the Rossendorf tandem accelerator was used. Only the central $2 \times 2 \text{ cm}^2$ (0.33 MeV) or $2 \times 3 \text{ cm}^2$ (2.4 MeV, 10 MeV) part of the wafers were implanted allowing the investigation of gettering and non-gettered material on the same wafer. Post-implantation annealing in dry nitrogen was performed by a furnace at 1000°C for 1 h (FA) and by rapid thermal annealing for 30 s at 1100°C (RTA1), 1250°C (RTA2) and 1350°C (RTA3).

The gate oxide layer on the front side was then thinned to about 70 nm by chemical etching to remove that part of the oxide layer which received most of the CH_4 and the other impurities during vacuum processing. Aluminium contacts were produced on the front side by photolithography (0.5 mm dots) and on the backside (full area). The contacts were subsequently annealed at 450°C for 30 min in dry nitrogen. Capacitance-voltage (C/V) and capacitance-time (C/t) measurements were used to evaluate the doping density and the

* SKORUPA, W., KÖGLER, R., SCHMALZ, K., and BARTSCH, H.: to be published